

ADAPTIVE PID CONTROL WITH PITCH MOMENT REJECTION FOR REDUCING UNWANTED VEHICLE MOTION IN LONGITUDINAL DIRECTION

Fauzi bin Ahmad¹, Khisbullah Hudha²,
Hishamuddin Jamaluddin³

^{1,2}Smart Material and Automotive Control (SMAC) Group,
Faculty of Mechanical Engineering,
Universiti Teknikal Malaysia Melaka, Hang Tuah Jaya,
76100 Durian Tunggal, Melaka, MALAYSIA

³Faculty of Mechanical Engineering,
Universiti Teknologi Malaysia (UTM)
81310 UTM Skudai, Johor, Malaysia

Email: ¹m040710003@student.utm.edu.my,
khisbullah@utm.edu, hishamj@fkm.utm.my

ABSTRACT

This manuscript provides a detailed derivation of a full vehicle model, which may be used to simulate the behavior of a vehicle in longitudinal direction. The dynamics of a 14 degrees of freedom (14-DOF) vehicle model are derived and integrated with an analytical tire dynamics namely Calspan tire model. The full vehicle model is then validated experimentally with an instrumented experimental vehicle based on the driver input from brake or throttle pedals. Several transient handling tests are performed, namely sudden acceleration and sudden braking test. Comparisons of the experimental result and model response with sudden braking and throttling imposed motion are made. The results of model validation show that the trends between simulation results and experimental data are almost similar with acceptable error. An adaptive PID control strategy is then developed on the validated full vehicle model to reduce unwanted vehicle motions during sudden braking and throttling maneuver. The results show that the proposed control structure is able to significantly improve the dynamic performance of the vehicle during sudden braking and sudden acceleration under various conditions. The proposed controller will be used to investigate the benefits of a pneumatically actuated active suspension system for reducing unwanted vehicle motion in longitudinal direction

KEYWORDS: *active suspension, dive and squat, 14 D.O.F. vehicle model, adaptive PID.*

1.0 INTRODUCTION

It is deemed necessary and useful to isolate disturbance elements that are prevalent in many mechanical systems. A clear example can be seen in an automotive system in which the passengers of a car should ideally be isolated from vibration or shaking effects of the car's body when the car hits a bump, cornering and braking. Referring to the characteristic of the vehicle's movement in longitudinal direction, the vehicle will dive forward when brake is applied. This is due to the fact that, inertia will cause a shift in the vehicle's center of gravity and weight will be transferred from the rear tires to the front tires. Similarly, the vehicle will squat to the rear when throttle input is applied. This is due to the weight transfer from the front to the rear. Both dive and squat are unwanted vehicle motions known as vehicle pitching (Ahmad *et.al.*, 2008a); (Ahmad *et.al.*, 2008b) and (Fenchea, 2008). This motion will cause the vehicle becomes unstable, lack of handling performance, out of control and moreover may cause an accident (Bahouth, 2005). Although this problem is worse, the common passive suspension cannot be controlled to give energy to suppress the weight transfers that cause moment. It is because the spring damper elements are generally fixed and are chosen based on the design requirement of the vehicle (Priyandoko *et.al.*, 2005).

To solve the problems, a considerable amount of works have been carried out to solve the problem both theoretically and experimentally (Alleyne and handrick1995; Lin and Kennelkopoulus, 1997). Through the combination of mechanical, electrical and hydraulic components, a wide range of controllable suspension systems have been developed varying in cost, sophistication and effectiveness. In general, these systems can be classified into three categories: semi-active suspensions (Gao *et.al.*, 2006), active anti-roll bars (Sampson *et.al.*, 2000) and active suspensions (Weeks *et.al.*, 2000; Sam *et.al.*, 2005). A semi active suspension is a passive system with controlled components usually the orifice or the fluid viscosity, which is able to adjust the stiffness of the damper. The active anti-roll bar system consists of an anti-roll bar mounted in the body and two actuators on each axle to cancel out the unwanted body motion. While the active suspension system is a controllable suspension that had the ability to add energy into the system, as well as store and dissipate it.

Investigation of active suspension systems for car models is recently increasing mostly because, they offer better riding comfort to passengers of high-speed ground transportation compared to passive and semi-active suspension systems. The research of active suspension systems

are derived by optimal control theory on the assumption that the car model is described by a linear or approximately linear system whose performance index is given in the quadratic form of the state variables and the (Donahue, 2001); (Sampson *et.al.*, 2002); (Sampson *et.al.*, 2003a); (Sampson *et.al.*, 2003b); (Karnopp, 1995); (Sam, 2006) and (Gao *et.al.*, 2006). However, nonlinear and intelligent active suspension systems are proposed for complicated models with no negligibly strong non-linearity and uncertainty. Numerical and experimental results showed that such active suspension systems give relatively more satisfactory performance, but need more increasing loads to achieve active control, compared with the linear active suspension systems (Yoshimura *et.al.*, 1997a; Yoshimura *et.al.*, 1997b; Yoshimura *et.al.*, 2003); Yoshimura and Watanabe, 2003; Labaryade *et.al.*, 2004; Kruczek *et.al.*, 2004); (Toshio and Atsushi, 2004)and (Yoshimura *et.al.* 2001). Some of the studies used 4-DOF vehicle model (Campos *et.al.*, 1999; Vaughan *et.al.*, 2003), and 7-DOF vehicle model has been investigated by Ikanega *et.al.*, (2000), and Zhang *et.al.*, (2004)

The exploration of the effectiveness active suspension system on real vehicle has been lead by Lotus Company at early 1980s. The company proposed a hydraulic active suspension system as a means to improved cornering in racing cars and come out with a new electro-hydraulic active suspension that is used in Lotus Excel model in 1985, but this was never offered to public (Watton *et.al.*, 2001). Six years after that, Nissan Motor Company produce a new type of luxury car that included two options joined namely traction control system and the world's first Full-Active Suspension (FAS). It used hydraulic actuators as the controllable suspension and used 10 sensors to counteract body lean, nose lift and nose dive, and fore/aft pitch on wavy surfaces (Trevett 2002). Beside that Mercedes Company used Hydraulic system to eliminate body roll called Active Body Control system (ABC). In this application the conventional spring-damper unit is mounted in series with the fluid chamber. When the car is cornering, the springs on the outer side of the corner will be compressed and at the same time the fluid chamber will be filled to compensate for the compression of the spring. In the same case, BMW company also used a hydraulic system to prevent body roll namely Dynamic Drive. The hydraulic system is used as the element in the anti roll bar that can supply a torque to each side of the anti roll bar (Ficher and Isermann 2004; Kadir 2009).

Since the hydraulic system is widely used as the active suspension, Citroen Company tries to make a difference by developing an active suspension base on the combination of the hydraulic and pneumatic system namely Hydractive Suspension System and then implemented it

into the Citroen Xantia Model 1989 (Martens 2005). Furthermore, Bose, known for its high-performance audio products, has developed an active suspension system which uses linear electric motors that replace the conventional spring-damper unit to produce the force required for eliminating body roll and pitch. The improvement in ride quality and the ability to suppress roll and pitch comes at an expense of energy consumption. However it contrasts to a hydraulic active suspension because the linear motor also can function as a generator. This means that, when the motor has to produce a force in the opposite direction of its velocity, energy can be generated where normally it would be dissipated by a conventional damper (Kadir, 2009).

The extensive research on the active suspension have resulted many control strategies. The control strategies that have been proposed to control the active suspension system may be loosely grouped into linear, nonlinear, hybrid and intelligent control approaches. The linear control strategies are mainly based on the optimal control theory such as LQR, LQG, LTR and H-infinity and are capable of minimizing a defined performance index. Application of the LQR method in active suspension system has been proposed by Hrovat (1988); Tseng and Hrovat (1990); Esmailzadeh and Taghirad (1996); Sam *et.al.*, (2000); and Su *et.al.*, (2008). The non-linear control strategies that have been applied in controlling active suspension are Fuzzy logic control used by Toshio and Itaru (2005); March and Shin (2007); and Yoshimura *et.al.*, (1999) and Sliding Mode Control (SMC) by Park and Kim (1998); Decarlo *et.al.*, (1998) and Sam *et.al.*, (2005). In terms of hybrid control strategies, PID Fuzzy Logic Neural Network (NN) and Genetic Algorithm (GA) have been applied to the active suspension system such as GA based PID proposed by Feng *et.al.*, (2003) and Sliding Mode Fuzzy control technique proposed by Ting *et.al.*, (1995). At the side of that, the intelligent control approaches have also been widely used which resulted many strategy like Fuzzy reasoning and a disturbance observer (Toshio and Itaru, 2005) and adaptive Fuzzy active force control (Mailah and Priyandoko, 2007).

Sparked with technological sophistication nowadays, a pneumatically actuated active suspension (PAAS) system is proposed. The proposed PAAS system is used to minimize the effects of unwanted pitch and vertical body motions of the vehicle in the presence of braking or throttle input from the driver. Like those stated, the proposed active suspension system is the system in which the passive suspension system is augmented by pneumatic actuators that supply additional external forces. The system is developed by using four units of pneumatic systems that are installed between lower arms and vehicle body parallel with

passive suspension. The reason of using the pneumatic system is due to the cheap cost for implementing in the real vehicle, the availability of the air without cost to pay and the compressibility of the air that can be used as the medium to transmit force. The proposed control strategy for the PAAS system is the combination of Adaptive PID (APID) based feedback control and pitch moment rejection based feed forward control (Stillwel *et.al.*, 1999; Lee *et.al.*, 2001; Sedaghati, 2006; Fialho and Balas, 2002). Feedback control is used to minimize unwanted body pitch motions, while the feed forward control is intended to reduce the unwanted weight transfer during braking and throttle maneuvers. The forces produced by the proposed control structure are used as the target forces by the four unit pneumatic actuators. The reason of using adaptive control based PID controller is because the PID controller has already been proven effective in many applications where it is easy to maintain and easy to implement in the Online Famos.

The proposed control structure is implemented on a validated full vehicle model. The full vehicle model can be approximately described as a 14-DOF system subject to excitation from braking and throttling inputs. It consists of 7-DOF vehicle ride model and 7-DOF vehicle handling model coupled with Calspan tire model (Kasprzak *et.al.*, 2006; Kadir *et.al.*, 2008; Ahmad *et.al.*, 2008c; Hudha *et.al.*, 2008). MATLAB-SIMULINK software is chosen as a computer simulation tool used to simulate the vehicle dynamics behavior and evaluate the performance of the control structure. In order to verify the effectiveness of the proposed controller, passive system and active system with PID controller without pitch moment rejection are selected as the benchmark

This paper is organized as follows: The first section contains the introduction and the review of some related works, followed by mathematical derivations of 14-DOF full vehicle model with Calspan tire model in the second section. The third section presents the proposed control structure for the pneumatically actuated active suspension system. The following section explains about the validation of 14-DOF vehicle model with the data obtained from instrumented experimental vehicle. The fifth section presents the performance evaluation of the proposed control structure. The last section contains some conclusion.

2.0 FULL VEHICLE MODEL WITH CALSPAN TIRE MODEL

The full-vehicle model of the passenger vehicle considered in this study consists of a single sprung mass (vehicle body) connected to four unsprung masses and is represented as a 14-DOF system. The sprung

mass is represented as a plane and is allowed to pitch, roll and yaw as well as to displace in vertical, lateral and longitudinal directions. The unsprung masses are allowed to bounce vertically with respect to the sprung mass. Each wheel is also allowed to rotate along its axis and only the two front wheels are free to steer.

2.1 Modeling Assumptions

Some of the modeling assumptions considered in this study are as follows: The vehicle body is lumped into a single mass which is referred to as the sprung mass, aerodynamic drag force is ignored, and the roll centre is coincident with the pitch centre and is located just below the body center of gravity. The suspensions between the sprung mass and unsprung masses are modeled as passive viscous dampers and spring elements. Rolling resistance due to passive stabilizer bar and body flexibility are neglected. The vehicle remains grounded at all times and the four tires never lost contact with the ground during maneuvering. A 4-degree-tilt angle of the suspension system towards vertical axis is neglected ($\cos \theta = 0.998 \approx 1$). The tire's vertical behavior is represented as a linear spring without damping, whereas the lateral and longitudinal behaviors are represented with Calspan model. Steering system is modeled as a constant ratio and the effect of steering inertia is neglected.

2.2 Vehicle Ride Model

The vehicle ride model is represented as a 7-DOF system. It consists of a single sprung mass (car body) connected to four unsprung masses (front-left, front-right, rear-left and rear-right wheels) at each corner. The sprung mass is free to heave, pitch and roll while the unsprung masses are free to bounce vertically with respect to the sprung mass. The suspensions between the sprung mass and unsprung masses are modeled as passive viscous dampers and spring elements, while, the tires are modeled as simple linear springs without damping. For simplicity, all pitch and roll angles are assumed to be small. A similar model was used by Ikanega (2000).

Referring to FIGURE 1, the force balance on sprung mass is given as

$$F_{fl} + F_{fr} + F_{rl} + F_{rr} + F_{pfl} + F_{pfr} + F_{prl} + F_{prr} = m_s \ddot{Z}_s \quad (1)$$

where,

- F_{fl} = suspension force at the front left corner
- F_{fr} = suspension force at the front right corner
- F_{rl} = suspension force at the rear left corner
- F_{rr} = suspension force at the rear right corner
- m_s = sprung mass weight
- \ddot{Z}_s = sprung mass acceleration at the body centre of gravity
- $F_{pfl}; F_{pfr}; F_{prl}; F_{prr}$ = pneumatic actuator forces at front left, front right, rear left and rear right corners, respectively.

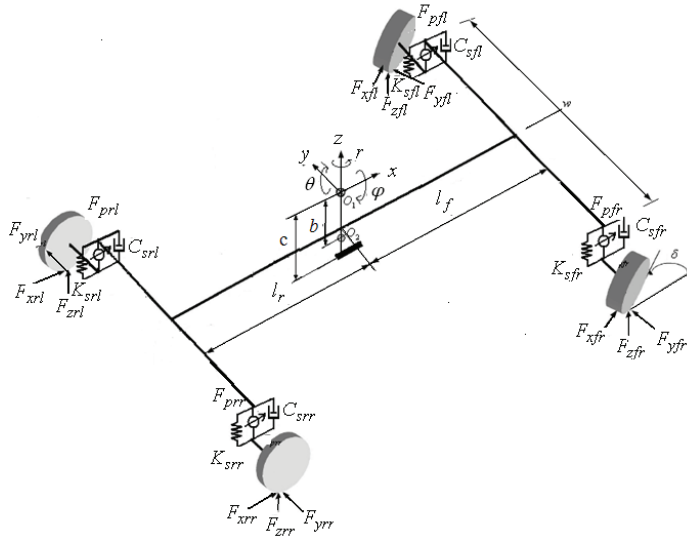


FIGURE 1: A 14-DOF Full vehicle ride and handling model

The suspension force at each corner of the vehicle is defined as the sum of the forces produced by suspension components namely spring force and damper force as the followings

$$\begin{aligned}
 F_{fl} &= K_{s,fl}(Z_{u,fl} - Z_{s,fl}) + C_{s,fl}(\dot{Z}_{u,fl} - \dot{Z}_{s,fl}) \\
 F_{fr} &= K_{s,fr}(Z_{u,fr} - Z_{s,fr}) + C_{s,fr}(\dot{Z}_{u,fr} - \dot{Z}_{s,fr}) \\
 F_{rl} &= K_{s,rl}(Z_{u,rl} - Z_{s,rl}) + C_{s,rl}(\dot{Z}_{u,rl} - \dot{Z}_{s,rl}) \\
 F_{rr} &= K_{s,rr}(Z_{u,rr} - Z_{s,rr}) + C_{s,rr}(\dot{Z}_{u,rr} - \dot{Z}_{s,rr})
 \end{aligned}
 \tag{2}$$

where,

- $K_{s,fl}$ = front left suspension spring stiffness
- $K_{s,fr}$ = front right suspension spring stiffness
- $K_{s,rr}$ = rear right suspension spring stiffness
- $K_{s,rl}$ = rear left suspension spring stiffness
- $C_{s,fr}$ = front right suspension damping
- $C_{s,fl}$ = front left suspension damping
- $C_{s,rr}$ = rear right suspension damping

- $C_{s,rl}$ = rear left suspension damping
- $Z_{u,fr}$ = front right unsprung masses displacement
- $Z_{u,fl}$ = front left unsprung masses displacement
- $Z_{u,rr}$ = rear right unsprung masses displacement
- $Z_{u,rl}$ = rear left unsprung masses displacement
- $\dot{Z}_{u,fr}$ = front right unsprung masses velocity
- $\dot{Z}_{u,fl}$ = front left unsprung masses velocity
- $\dot{Z}_{u,rr}$ = rear right unsprung masses velocity
- $\dot{Z}_{u,rl}$ = rear left unsprung masses velocity

The sprung mass position at each corner can be expressed in terms of bounce, pitch and roll given as;

$$\begin{aligned}
 Z_{s,fl} &= Z_s - a \sin \theta + 0.5w \sin \varphi \\
 Z_{s,fr} &= Z_s - a \sin \theta - 0.5w \sin \varphi \\
 Z_{s,rl} &= Z_s + b \sin \theta + 0.5w \sin \varphi \\
 Z_{s,rr} &= Z_s + a \sin \theta - 0.5w \sin \varphi
 \end{aligned} \tag{3}$$

It is assumed that all angles are small, therefore Eq. (3) becomes;

$$\begin{aligned}
 Z_{s,fl} &= Z_s - a\theta + 0.5w\varphi \\
 Z_{s,fr} &= Z_s - a\theta - 0.5w\varphi \\
 Z_{s,rl} &= Z_s + b\theta + 0.5w\varphi \\
 Z_{s,rr} &= Z_s + a\theta - 0.5w\varphi
 \end{aligned} \tag{4}$$

where,

- a = distance between front of vehicle and C.G. of sprung mass
- b = distance between rear of vehicle and C.G. of sprung mass
- θ = pitch angle at body centre of gravity
- φ = roll angle at body centre of gravity
- $Z_{s,fl}$ = front left sprung mass displacement
- $Z_{s,fr}$ = front right sprung mass displacement
- $Z_{s,rl}$ = rear left sprung mass displacement
- $Z_{s,rr}$ = rear right sprung mass displacement

By substituting Eq. (4) and its derivative (sprung mass velocity at each corner) into Eq. (2) and the resulting equations are then substituted into Eq. (1), the following equation is obtained ;

$$\begin{aligned}
 m_s \ddot{Z}_s = & -2(K_{s,f} + K_{s,r})Z_s - 2(C_{s,f} + C_{s,r})\dot{Z}_s + 2(aK_{s,f} - bC_{s,r})\dot{\theta} \\
 & + 2(aC_{s,f} - bC_{s,r})\dot{\theta} + K_{sf}Z_{u,fl} + C_{s,f}\dot{Z}_{u,fl} + K_{sf}Z_{u,fr} \\
 & + C_{s,f}\dot{Z}_{u,fr} + K_{sr}Z_{u,rl} + C_{s,r}\dot{Z}_{u,rl} + K_{sr}Z_{u,rr} + C_{s,r}\dot{Z}_{u,rr} \\
 & + F_{pfl} + F_{pfr} + F_{prl} + F_{pr}
 \end{aligned} \tag{5}$$

where,

- $\dot{\theta}$ = pitch rate at body centre of gravity
- Z_s = sprung mass displacement at body centre of gravity
- \dot{Z}_s = sprung mass velocity at body centre of gravity
- $K_{s,f}$ = spring stiffness of front suspension ($K_{s,fl} = K_{s,fr}$)
- $K_{s,r}$ = spring stiffness of rear suspension ($K_{s,rl} = K_{s,rr}$)
- $C_{s,f} = C_{s,fl} = C_{s,fr}$ = damping constant of front suspension
- $C_{s,r} = C_{s,rl} = C_{s,rr}$ = damping constant of rear suspension

Similarly, moment balance equations are derived for pitch θ ; and roll ϕ , and are given as ;

$$\begin{aligned}
 I_{yy}\ddot{\theta} = & 2(aK_{s,f} - bK_{s,r})Z_s + 2(aC_{s,f} - bC_{s,r})\dot{Z}_s - 2(a^2K_{s,f} + b^2K_{s,r})\dot{\theta} \\
 & - 2(a^2C_{s,f} + b^2C_{s,r})\dot{\theta} - aK_{s,f}Z_{u,fl} - aC_{s,f}\dot{Z}_{u,fl} - aK_{s,f}Z_{u,fr} \\
 & - aC_{s,f}\dot{Z}_{u,fr} + bK_{s,r}Z_{u,rl} + bC_{s,r}\dot{Z}_{u,rl} + bK_{s,r}Z_{u,rr} + bC_{s,r}\dot{Z}_{u,rr} \\
 & - (F_{pfl} + F_{pfr})l_f + (F_{prl} + F_{pr})l_r
 \end{aligned} \tag{6}$$

$$\begin{aligned}
 I_{xx}\ddot{\phi} = & -0.5w^2(K_{s,f} + K_{s,r})\phi - 0.5w^2(C_{s,f} + C_{s,r})\dot{\phi} + 0.5wK_{s,f}Z_{u,fl} \\
 & + 0.5wC_{s,f}\dot{Z}_{u,fl} - 0.5wK_{s,f}Z_{u,fr} - 0.5wC_{s,f}\dot{Z}_{u,fr} \\
 & + 0.5wK_{s,r}Z_{u,rl} + 0.5wC_{s,r}\dot{Z}_{u,rl} - 0.5wK_{s,r}Z_{u,rr} - 0.5wC_{s,r}\dot{Z}_{u,rr} \\
 & + (F_{pfl} + F_{prl})\frac{w}{2} - (F_{pfr} + F_{pr})\frac{w}{2}
 \end{aligned} \tag{7}$$

- $\ddot{\theta}$ = pitch acceleration at body centre of gravity
- $\ddot{\phi}$ = roll acceleration at body centre of gravity
- I_{xx} = roll axis moment of inertia
- I_{yy} = pitch axis moment of inertia
- w = wheel base of sprung mass

where,

$$\begin{aligned}
 m_u \ddot{Z}_{u,fl} = & K_{s,f}Z_s + C_{s,f}\dot{Z}_s - aK_{s,f}\theta - aC_{s,f}\dot{\theta} + 0.5wK_{s,f}\phi \\
 & + 0.5wC_{s,f}\dot{\phi} - (K_{s,f} + K_t)Z_{u,fl} - C_{s,f}\dot{Z}_{u,fl} + K_t Z_{r,fl} - F_{pfl}
 \end{aligned} \tag{8}$$

$$m_u \ddot{Z}_{u,fr} = K_{s,f} Z_s + C_{s,f} \dot{Z}_s - aK_{s,f} \theta - aC_{s,f} \dot{\theta} - 0.5wK_{s,f} \varphi - 0.5wC_{s,f} \dot{\varphi} - (K_{s,f} + K_t) Z_{u,fr} - C_{s,f} \dot{Z}_{u,fr} + K_t Z_{r,fr} - F_{pfr} \quad (9)$$

$$m_u \ddot{Z}_{u,rl} = K_{s,r} Z_s + C_{s,r} \dot{Z}_s + bK_{s,r} \theta + bC_{s,r} \dot{\theta} + 0.5wK_{s,r} \varphi + 0.5wC_{s,r} \dot{\varphi} - (K_{s,r} + K_t) Z_{u,rl} - C_{s,r} \dot{Z}_{u,rl} + K_t Z_{r,rl} - F_{prl} \quad (10)$$

$$m_u \ddot{Z}_{u,rr} = K_{s,r} Z_s + C_{s,r} \dot{Z}_s + aK_{s,r} \theta + bC_{s,r} \dot{\theta} - 0.5wK_{s,r} \varphi - 0.5wC_{s,r} \dot{\varphi} - (K_{s,r} + K_t) Z_{u,rr} - C_{s,r} \dot{Z}_{u,rr} + K_t Z_{r,rr} - F_{prr} \quad (11)$$

where,

$\ddot{Z}_{u,fr}$ = front right unsprung masses acceleration

$\ddot{Z}_{u,fl}$ = front left unsprung masses acceleration

$\ddot{Z}_{u,rr}$ = rear right unsprung masses acceleration

$\ddot{Z}_{u,rl}$ = rear left unsprung masses acceleration

$Z_{r,fr} = Z_{r,fl} = Z_{r,rr} = Z_{r,rl}$ = road profiles at front left, front right, rear right and rear left tires respectively

2.3 Vehicle Handling Model

The handling model employed in this paper is a 7-DOF system as shown in FIGURE 2. It takes into account three degrees of freedom for the vehicle body in lateral and longitudinal motions as well as yaw motion (r) and one degree of freedom due to the rotational motion of each tire. In vehicle handling model, it is assumed that the vehicle is moving on a flat road. The vehicle experiences motion along the longitudinal x -axis, the lateral y -axis, and the angular motions of yaw around the vertical z -axis. The motion in the horizontal plane can be characterized by the longitudinal and lateral accelerations, denoted by a_x and a_y respectively, and the velocities in longitudinal and lateral direction, denoted by v_x and v_y respectively.

Acceleration in longitudinal x -axis is defined as ;

$$\dot{v}_x = a_x + v_y \dot{r} \quad (12)$$

By summing all the forces in x -axis, longitudinal acceleration can be defined as ;

$$a_x = \frac{F_{xfl} \cos \delta + F_{yfl} \sin \delta + F_{xfr} \cos \delta + F_{yfr} \sin \delta + F_{xrl} + F_{xrr}}{m_t} \quad (13)$$

Similarly, acceleration in lateral y -axis is defined as ;

$$\dot{v}_y = a_y - v_x \dot{r} \quad (14)$$

By summing all the forces in lateral direction, lateral acceleration can be defined as ;

$$a_y = \frac{F_{yfl} \cos \delta - F_{xfl} \sin \delta + F_{yfr} \cos \delta - F_{xfr} \sin \delta + F_{yrl} + F_{yrr}}{m_t} \quad (15)$$

where F_{xij} and F_{yij} denote the tire forces in the longitudinal and lateral directions, respectively, with the index (i) indicating front (f) or rear (r) tires and index (j) indicating left (l) or right (r) tires. The steering angle is denoted by δ , the yaw rate by r and m_t denotes the total vehicle mass. The longitudinal and lateral vehicle velocities v_x and v_y can be obtained by the integration of \dot{v}_y and \dot{v}_x . They can be used to obtain the side slip angle, denoted by α . Thus, the slip angle of front and rear tires are found as ;

$$\alpha_f = \tan^{-1} \left(\frac{v_y + L_f r}{v_x} \right) - \delta_f \quad (16)$$

and

$$\alpha_r = \tan^{-1} \left(\frac{v_y - L_r r}{v_x} \right) \quad (17)$$

where, α_f and α_r are the side slip angles at the front and rear tires respectively. l_f and l_r are the distance between the front and rear tire to the body center of gravity respectively.

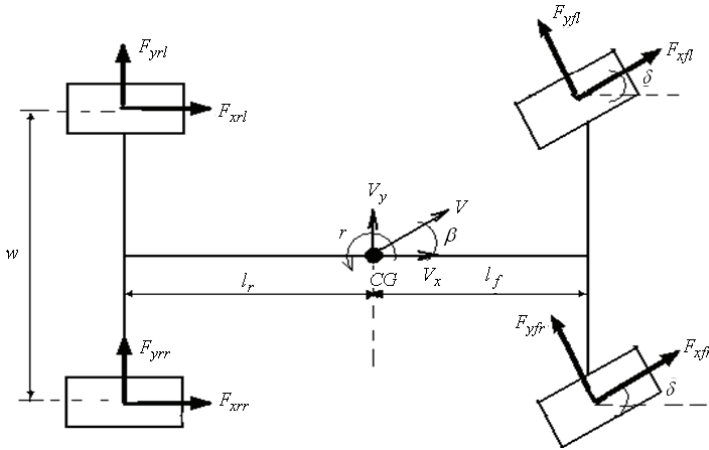


FIGURE 2: A 7-DOF vehicle handling model

To calculate the longitudinal slip, longitudinal component of the tire's velocity should be derived. The front and rear longitudinal velocity component is given by:

$$v_{wxf} = V_{tf} \cos \alpha_f \tag{18}$$

where, the speed of the front tire is,

$$V_{tf} = \sqrt{(v_y + L_f r)^2 + v_x^2} \tag{19}$$

the rear longitudinal velocity component is,

$$v_{wxr} = V_{tr} \cos \alpha_r \tag{20}$$

where, the speed of the rear tire is,

$$V_{tr} = \sqrt{(v_y + L_r r)^2 + v_x^2} \tag{21}$$

then, the longitudinal slip ratio of the front tire is,

$$S_{af} = \frac{v_{wxf} - \omega_f R_w}{v_{wxf}} \text{ under braking conditions} \tag{22}$$

the longitudinal slip ratio of the rear tire is,

$$S_{ar} = \frac{v_{wxr} - \omega_r R_w}{v_{wxr}} \text{ under braking conditions} \quad (23)$$

where, ω_r and ω_f are angular velocities of the rear and front tires, respectively and r_w is the wheel radius. The yaw motion is also dependent on the tire forces F_{xij} and F_{yij} as well as on the self-aligning moments, denoted by M_{zij} acting on each tire:

$$\begin{aligned} \ddot{r} = \frac{1}{J_z} [& \frac{w}{2} F_{yfl} \cos \delta - \frac{w}{2} F_{yfr} \cos \delta + \frac{w}{2} F_{xrl} - \frac{w}{2} F_{xrr} + \frac{w}{2} F_{yfl} \sin \delta - \\ & \frac{w}{2} F_{yfr} \sin \delta - l_r F_{yrl} - l_r F_{yrr} + l_f F_{yfl} \cos \delta + l_f F_{yfr} \cos \delta - l_f F_{xfl} \sin \delta - \\ & l_f F_{xfr} \sin \delta + M_{zfl} + M_{zfr} + M_{zrl} + M_{zrr}] \end{aligned} \quad (24)$$

where, J_z is the moment of inertia around the z-axis. The roll and pitch motion depend very much on the longitudinal and lateral accelerations. Since only the vehicle's body undergoes roll and pitch, the sprung mass, denoted by m_s has to be considered in determining the effects of handling on pitch and roll motions as the following:

$$\ddot{\phi} = \frac{-m_s c a_y + \phi(m_s g c - k_\phi) + \dot{\phi}(-\beta_\phi)}{J_{sx}} \quad (25)$$

$$\ddot{\theta} = \frac{-m_s c a_y + \theta(m_s g c - k_\theta) + \dot{\theta}(-\beta_\theta)}{J_{sy}} \quad (26)$$

where, c is the height of the sprung mass center of gravity to the ground, g is the gravitational acceleration and $k_\phi, \beta_\phi, k_\theta$ and β_θ are the damping and stiffness constant for roll and pitch, respectively. The moments of inertia of the sprung mass around x-axes and y-axes are denoted by j_{sx} and j_{sy} respectively.

2.4 Braking and Throttling Torques

For the front and rear wheels, the sum of the torque about the axis shown in FIGURE 3 are as follows:

$$F_{xf} R_w - T_{bf} + T_{af} = I_\omega \dot{\omega}_f \quad (27)$$

$$F_{xr} R_{\omega} - T_{br} + T_{ar} = I_{\omega} \dot{\omega}_r \quad (28)$$

where ω_f and ω_r are the angular velocity of the front and rear wheels, I_{ω} is the inertia of the wheel about the axle, R_{ω} is the wheel radius, T_{bf} and T_{br} are the applied braking torques, and T_{af} and T_{ar} are the applied throttling torques for the front and rear wheels

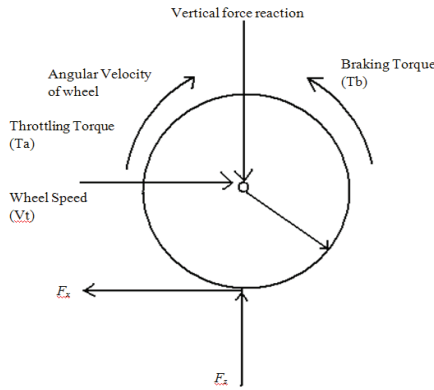


FIGURE 3: Free body diagram of a wheel

2.5 Simplified Calspan Tire Model

The tire model considered in this study is Calspan model as described in Szostak *et.al.* (1988). Calspan model is able to describe the behavior of a vehicle in any driving scenario including inclement driving conditions which may require severe steering, braking, accelerating, and other driving related operations (Kadir *et.al.*, 2008). The longitudinal and lateral forces generated by a tire are functions of the slip angle and longitudinal slip of the tire relative to the road. The previous theoretical developments in Szostak *et.al.* (1988) lead to a complex, highly non-linear composite force as a function of composite slip. It is convenient to define a saturation function, $f(\sigma)$, to obtain a composite force with any normal load and coefficient of friction values (Singh *et.al.*, 2002). The polynomial expression of the saturation function is presented by:

$$f(\sigma) = \frac{F_c}{\mu F_z} = \frac{C_1 \sigma^3 + C_2 \sigma^2 + (4/\pi) \sigma}{C_1 \sigma^3 + C_2 \sigma^2 + C_4 \sigma + 1} \quad (29)$$

where, C_1 , C_2 , C_3 and C_4 are constant parameters fixed to the specific tires. The tire's contact patch lengths are calculated using the following two equations:

$$ap_0 = \frac{0.0768 \sqrt{F_z F_{ZT}}}{T_w (T_p + 5)} \tag{30}$$

$$ap = \left(1 - \frac{K_a F_x}{F_z} \right) \tag{31}$$

Where ap is the tire’s contact patch, T_w is the tread width, and T_p is the tire pressure. The values of F_{ZT} and $K\alpha$ are the tire’s contact patch constants. The lateral and longitudinal stiffness coefficient (K_s and K_c respectively) are a function of the tire contact patch’s length and normal load of the tire as expressed as follows:

$$K_s = \frac{2}{ap_0^2} \left(A_0 + A_1 F_z - \frac{A_1 F_z^2}{A_2} \right) \tag{32}$$

$$K_c = \frac{2}{ap_0^2} F_z (CS / FZ) \tag{33}$$

Where the values of A_0 , A_1 , A_2 and CS/FZ are stiffness constants and can be found in Table 2. Then, the composite slip calculation becomes:

$$\sigma = \frac{\pi ap^2}{8\mu_0 F_z} \sqrt{K_s^2 \tan^2 \alpha + K_c^2 \left(\frac{s}{1-s} \right)^2} \tag{34}$$

μ_0 is a nominal coefficient of friction and has a value of 0.85 for normal road condition, 0.3 for wet road condition, and 0.1 for icy road condition. Given the polynomial saturation function, lateral and longitudinal stiffness, the normalized lateral and longitudinal forces are derived by resolving the composite force into the side slip angle and longitudinal slip ratio components:

$$\frac{F_y}{\mu F_z} = \frac{f(\sigma) K_s \tan \alpha}{\sqrt{K_s^2 \tan^2 \alpha + K_c'^2 S^2}} + Y_\gamma \gamma \tag{35}$$

$$\frac{F_x}{\mu F_z} = \frac{f(\sigma) K_c' S}{\sqrt{K_s^2 \tan^2 \alpha + K_c'^2 S^2}} \tag{36}$$

Lateral force has an additional component due to the tire’s chamber angle, γ , which is modeled as a linear effect. Under significant

maneuvering conditions with large lateral and longitudinal slip, the force converges to a common sliding friction value. In order to meet this criterion, the longitudinal stiffness coefficient is modified at high slips to transition to lateral stiffness coefficient as well as the coefficient of friction defined by the parameter K_μ .

$$K'_c = K_c + (K_s - K_c) \sqrt{\sin^2 \alpha + S^2 \cos^2 \alpha} \tag{37}$$

$$\mu = \mu_0 (1 - K_\mu) \sqrt{\sin^2 \alpha + S^2 \cos^2 \alpha} \tag{38}$$

2.6 Description of the simulation model

The vehicle dynamics model is developed based on the mathematical equations from the previous vehicle handling equations by using MATLAB SIMULINK software. The relationship between handling model, ride model, tire model, slip angle and longitudinal slip are clearly described in FIGURE 4. In this model there are two inputs that can be used in the dynamic analysis of the vehicle namely torque input and steering input which come from the driver. It simply explains that the model created is able to perform the analysis for longitudinal and lateral direction.

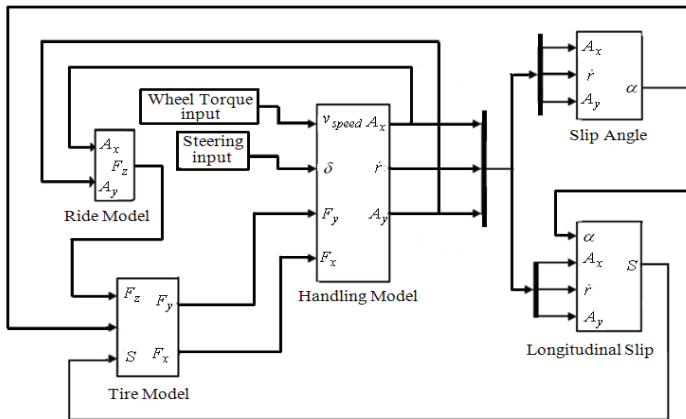


FIGURE 4: Full Vehicle Model in Matlab SIMULINK

3.0 ACTIVE CONTROL SYSTEM DESIGN

The controller structure consists of an inner loop controller to reject the unwanted weight transfer and an outer loop controller to stabilize heave and pitch responses due to pitch torque input from the driver. An

input decoupling transformation is placed between the inner and outer loop controllers that blend the inner loop and outer loop controllers. The outer loop controller provides the ride control that isolates the vehicle's body from vertical and rotational vibrations induced by pitch torque input. The inner loop controller provides the weight transfer rejection control that maintains load-leveling and load distribution during vehicle maneuvers. The proposed control structure is shown in FIGURE 5.

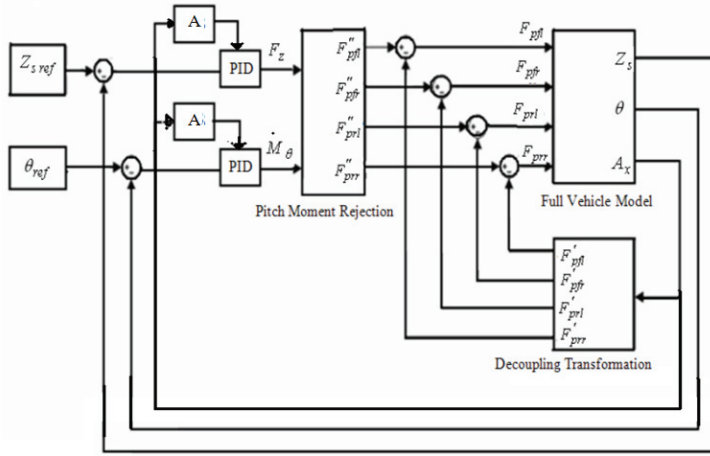


FIGURE 5: The Proposed Control Structure for Active Suspension System

3.1 Decoupling Transformation

The outputs of the outer loop controller are vertical forces to stabilize body bounce (F_z) and moment to stabilize pitch (M_θ). These forces and moments are then distributed into target forces of the four pneumatic actuators produced by the outer loop controller. Distribution of the forces and moments into target forces of the four pneumatic actuators is performed using decoupling transformation subsystem. The outputs of the decoupling transformation subsystem namely the target forces for the four pneumatic actuators are then subtracted with the relevant outputs from the inner loop controller to produce the ideal target forces for the four pneumatic actuators. Decoupling transformation subsystem requires an understanding of the system dynamics in the previous section. From equations (5), (6) and (7), equivalent forces and moments for heave, pitch and roll can be defined as:

$$F_z = F''_{pfl} + F''_{pfr} + F''_{prl} + F''_{prf} \tag{39}$$

$$M_{\theta} = -F''_{pfl} l_f - F''_{pfr} l_f + F''_{prl} l_r + F''_{prr} l_r \quad (40)$$

$$M_{\varphi} = F''_{pfl} \left(\frac{w}{2}\right) - F''_{pfr} \left(\frac{w}{2}\right) + F''_{prl} \left(\frac{w}{2}\right) - F''_{prr} \left(\frac{w}{2}\right) \quad (41)$$

where $F''_{pfl}, F''_{pfr}, F''_{prl}$ and F''_{prr} are the pneumatic forces which are produced by the outer loop controller in the front left, front right, rear left and rear right corners, respectively. In the case of the vehicle input that comes from the brake torque, the roll moment can be neglected. Equations (39), (40) and (41) can be rearranged in a matrix format as follows:

$$\begin{bmatrix} f_z(t) \\ M_{\theta}(t) \\ M_{\varphi}(t) \end{bmatrix} = \begin{bmatrix} 1 & 1 & 1 & 1 \\ -L_f & -L_f & L_r & L_r \\ \frac{w}{2} & -\frac{w}{2} & \frac{w}{2} & -\frac{w}{2} \end{bmatrix} \begin{bmatrix} F''_{pfl} \\ F''_{pfr} \\ F''_{prl} \\ F''_{prr} \end{bmatrix} \quad (42)$$

For a linear system of equations $\mathbf{y}=\mathbf{C}\mathbf{x}$, if $\mathbf{C} \in \mathfrak{R}^{m \times n}$ has a full row rank, then a right inverse \mathbf{C}^{-1} such as $\mathbf{C}^{-1}\mathbf{C} = \mathbf{I}^{m \times m}$ still exist. The right inverse can be computed using . Thus, the inverse relationship of equation (42) can be expressed as ;

$$\begin{bmatrix} F''_{pfl} \\ F''_{pfr} \\ F''_{prl} \\ F''_{prr} \end{bmatrix} = \begin{bmatrix} \frac{l_r}{2(l_f + l_r)} & -\frac{1}{2(l_f + l_r)} & \frac{1}{2w} \\ \frac{l_r}{2(l_f + l_r)} & -\frac{1}{2(l_f + l_r)} & -\frac{1}{2w} \\ \frac{l_f}{2(l_f + l_r)} & \frac{1}{2(l_f + l_r)} & \frac{1}{2w} \\ \frac{l_f}{2(l_f + l_r)} & \frac{1}{2(l_f + l_r)} & -\frac{1}{2w} \end{bmatrix} \begin{bmatrix} F_z \\ M_{\theta} \\ M_{\varphi} \end{bmatrix} \quad (43)$$

3.2 Pitch Moment Rejection Loop

In the outer loop controller, APID control is applied for suppressing both body vertical displacement and body pitch angle. The inner loop controller of pitch moment rejection control is described as follows: during throttling and braking, a vehicle will produce a force, namely throttling force and braking force respectively at the body center of gravity. The throttling force generates a pitch moment causing the body

center of gravity to shift backward as shown in FIGURE 6 and vice versa when braking input is applied. Shifting the body center of gravity causes a weight transfer from an axle to the other axle. By defining the distance between the body center of gravity and the pitch pole is H_{pc} , pitch moment is defined by:

$$M_p = M(a_x)H_{pc} \tag{44}$$

In case of braking, the two pneumatic actuators installed in the front axle have to produce the necessary forces to cancel out the unwanted pitch moments, whereas the forces of the two pneumatic actuators at the rear axle will act in the opposite. Pneumatic forces that cancel out pitch moment in each corner due to braking input are defined as:

$$F'_{pfr} = F'_{pfl} = \frac{M_p(a_x)H_{pc}}{L_f} \text{ and } F'_{prl} = F'_{prr} = -\left(\frac{M_p(a_x)H_{pc}}{L_f}\right) \tag{45}$$

Whereas, pneumatic forces that cancel out pitch moment in each corner for throttle input can be defined as:

$$F'_{prl} = F'_{prr} = \frac{M_p(a_x)H_{pc}}{L_r} \text{ and } F'_{pfl} = F'_{pfr} = -\left(\frac{M_p(a_x)H_{pc}}{L_r}\right) \tag{46}$$

where,

F_{pfl} = target force of pneumatic system at the front left corner produced by inner loop controller

F_{pfr} = target force of pneumatic system at the front right corner produced by inner loop controller

F_{prl} = target force of pneumatic system at the rear left corner produced by inner loop controller

F_{prr} = target force of pneumatic system at the rear right corner produced by inner loop controller

The ideal target forces for each pneumatic actuator are defined as the target forces produced by the outer loop controller subtracted with the respective target forces produced by inner loop controller as following:

$$F_{pfl} = F''_{pfl} - F'_{pfl} \tag{47}$$

$$F_{pfr} = F''_{pfr} - F'_{pfr} \tag{48}$$

$$F_{prl} = F''_{prl} - F'_{prl} \tag{49}$$

$$F_{prr} = F''_{prr} - F'_{prr} \tag{50}$$

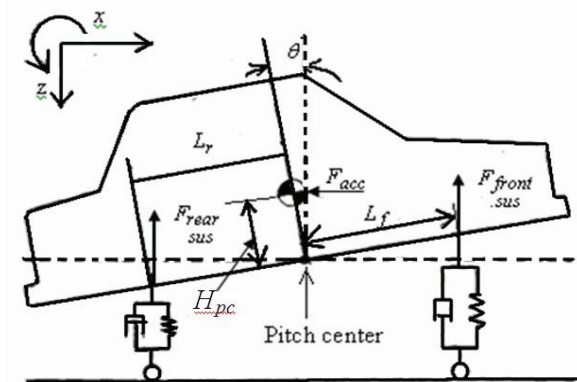


FIGURE 6: Free body diagram for pitch motion.

3.3 Adaptive PID Control

From many previous researches, it has been identified that PID controller is already proven effective in many applications but unable to continuously vary with the variation condition. Because of that, an adaptive PID controller is needed. The APID controller that is applied in the suspension system is shown in FIGURE 6 and can mathematically be described as the following equations ;

$$F_z(t) = K_p(t) e(t) + k_i(t) \int e(t) dt + k_d(t) \frac{d}{dt} e(t) \tag{51}$$

Where $e(t) = Z_s ref(t) - Z_s(t)$; and the proportional gain, $k_p(t)$, integral gain, $k_i(t)$ and derivative gain, $k_d(t)$ are the functions of the position longitudinal acceleration $A_x(t)$. The proportional gain $k_p(t)$ as the function of the longitudinal acceleration $A_x(t)$ can be expressed mathematically as follows;

$$k_p(t) = 162.3 A_x(t) + 2231 \tag{52}$$

The integral gain $k_i(t)$ in equation (53) as a function of position

longitudinal acceleration $A_x(t)$ can be expressed mathematically as follows:

$$k_i(t) = -131.2 A_x(t) + 720.6 \quad (53)$$

The derivative gain $k_d(t)$ in equation (53) as a function of longitudinal acceleration $A_x(t)$ can be expressed mathematically as follows:

$$k_d(t) = -106.0 A_x(t) + 1660 \quad (54)$$

On the other hand the same function is used for stabilizing the body pitch and it can be expressed mathematically as follows:

$$M_\theta(t) = K_p(t) e(t) + k_i(t) \int e(t) dt + k_d(t) \frac{d}{dt} e(t) \quad (55)$$

Where $e(t) = \theta_{ref}(t) - \theta(t)$ and the proportional gain, $k_p(t)$, integral gain, $k_i(t)$ and derivative gain, $k_d(t)$ are the function of the position longitudinal acceleration $A_x(t)$, where the proportional gain $k_p(t)$ are:

$$k_p(t) = 121.2 A_x(t) + 2015 \quad (56)$$

The integral gain $k_i(t)$ in equation (53) as a function of longitudinal acceleration $A_x(t)$ can be expressed mathematically as follows:

$$k_i(t) = -56.27 A_x(t) + 243.7 \quad (57)$$

The derivative gain $k_d(t)$ in equation (53) as a function of longitudinal acceleration $A_x(t)$ can be expressed mathematically as follows:

$$k_d(t) = -133.6 A_x(t) + 1261 \quad (58)$$

The constant values in the equations (51) to (58) are obtained from linearization of the controller gained with the value of longitudinal acceleration as discussed in Appendix. Before linearization is made, it is necessary to identify the PID controller parameters of all the input condition in simulation of sudden acceleration and sudden braking test.

In these conditions, the simulations have been made with 1Mpa, 3Mpa and 6Mpa brake pressure in sudden braking test, while 0.2, 0.6 and full step throttle for the sudden acceleration test. The controller parameters obtained from the tests are described in Table 1.

Table 1: PID controller parameters

Driver Input	Controller Parameter						Longitudinal Acceleration (G)
	Body Displacement (controller for F_z)			Body Pitch (controller for M_θ)			
	Kp	Ki	Kd	Kp	Ki	Kd	
1Mpa brake	800	700	1600	600	300	1500	-1.36
3Mpa brake	1000	1000	2000	1000	500	2000	-2.72
6Mpa brake	2000	2000	3000	1852	7000	2251	-8.2
0.2 step throttle	3000	100	500	2500	50	700	0.96
0.6 step throttle	1000	900	750	2700	57	800	2.89
full step throttle	5000	100	2500	30000	60	8000	4.8

4.0 VALIDATION OF 14 DOF VEHICLE MODEL USING INSTRUMENTED EXPERIMENTAL VEHICLE

To verify the full vehicle ride and handling model that have been derived, experimental works are performed using an instrumented experimental vehicle. This section provides the verification of ride and handling model using visual technique by simply comparing the trend of simulation results with experimental data using the same input signals. Validation or verification is defined as the comparison of model's performance with the real system. Therefore, the validation does not mean that the fitting of simulated data is exact as the measured data, but as gaining confidence that the vehicle handling simulation is giving insight into the behavior of the simulated vehicle reference. The tests data are also used to check whether the input parameters for the vehicle model are reasonable. In general, model validation can be defined as determining the acceptability of a model by using some statistical tests for deviance measured or subjectively using visual techniques reference.

4.1 Vehicle Instrumentation

The data acquisition system (DAS) is installed into the experimental vehicle to obtain the real vehicle reaction as to evaluate the vehicle's performance in terms of longitudinal acceleration, body vertical

acceleration and pitch rate. The DAS uses several types of transducers such as single axis accelerometer to measure the sprung mass and unsprung mass accelerations for each corner, tri-axial accelerometer to measure longitudinal, vertical and lateral accelerations at the body center of gravity, tri-axial gyroscopes for the pitch rate and wheel speed sensor to measure angular velocity of the tire. The multi-channel μ -MUSYCS system Integrated Measurement and Control (IMC) is used as the DAS system. Online FAMOS software as the real time data processing and display function is used to ease the data collection. The installation of the DAS and sensors to the experimental vehicle can be seen in FIGURE 7.

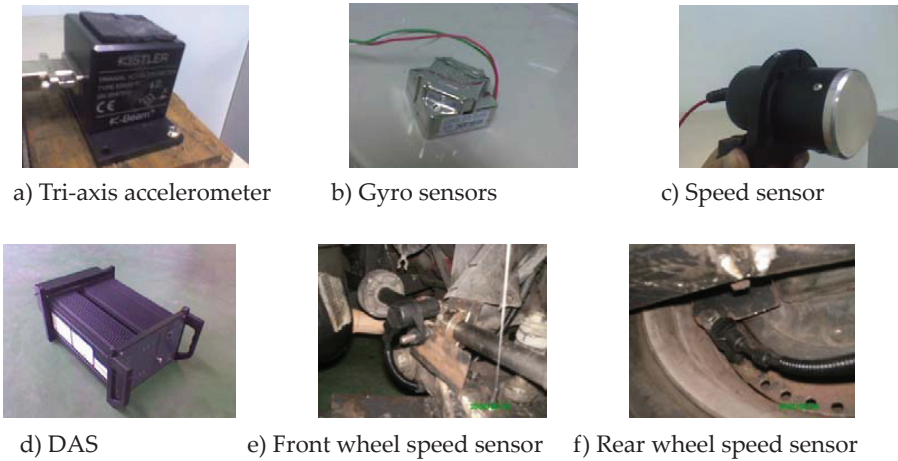


FIGURE 7: In-vehicle instrumentations

4.2 Experimental Vehicle

An instrumented experimental vehicle is developed to validate the full vehicle model. A Malaysian National car is used to perform sudden braking and sudden acceleration test, defined in (SAE J266, 1996). Note that the vehicle is 1300 cc and uses manual gear shift as the power terrain systems. The technical specifications of the vehicle are listed in Table 1.

TABLE 1: Experimental vehicle Parameter

Parameter	Value
Vehicle mass	920kg
Wheel base	2380mm
Wheel track	1340mm
Spring rate: Front:	30 N/mm
Rear:	30 N/mm
Damper rate : Front:	1000 N/msec ⁻¹
Rear:	1000 N/msec ⁻¹
Roll center	100
Center of gravity	550mm
Wheel radius	285mm

4.3 Validation Procedures

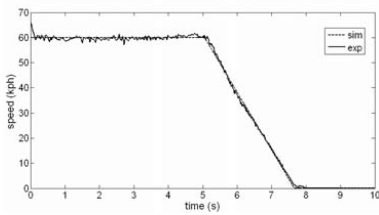
The dynamic response characteristics of a vehicle model that include longitudinal acceleration, longitudinal slip in each tire and pitch rate can be validated using experimental test through several handling test procedures namely sudden braking test and sudden acceleration test. Sudden braking test is intended to study transient response of the vehicle under braking input. In this case, the tests were conducted by accelerating the vehicle to a nominal speed of 60kph and activating the instrumentation package. The driver then applies the brake pedal hard enough to hold the pedal firmly until the vehicle stopped completely as shown in FIGURE 8(a). On the other hand, sudden acceleration test is used to evaluate the characteristics of the vehicle during a sudden increase of speed. In this study, the vehicle accelerated to a nominal speed of 40kph and activated the instrument package. The driver then manually applied the throttle pedal full step as required to make the vehicle accelerated immediately as shown in FIGURE 8(b).

4.4 Validation Results

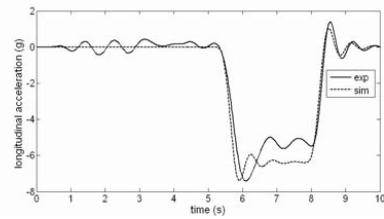
FIGURES 9 and 10 show a comparison of the results obtained using SIMULINK and experimental. In experimental works, all the experimental data are filtered to remove out any unintended data. It is necessary to note that the measured vehicle speed from the speed sensor is used as the input of simulation model. For the simulation model, tire parameters are obtained from Szostak *et.al.* (1988) and Singh *et.al.* (2002). The results of model verification for sudden braking test at 60 kph are shown in FIGURE 9. FIGURE 9(a) shows the vehicle speed applied for the test. It can be seen that the trends between simulation results and experimental data are almost similar with acceptable error. The small difference in magnitude between simulation and experimental results is due to the fact that, in an actual situation, it is indeed very hard for

the driver to maintain the vehicle in a perfect speed as compared to the result obtained in the simulation.

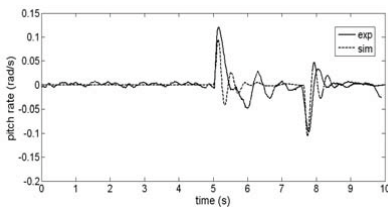
In terms of both longitudinal acceleration and pitch rate response, it can be seen that there are quite good comparisons during the initial transient phase as well as during the following steady state phase as shown in FIGURES 9(b) and (c) respectively. Longitudinal slip responses of the front tires also show satisfactory matches with only small deviation in the transition area between transient and steady state phases as shown in FIGURE 9(d) and (e). It can also be noted that the longitudinal slip responses to all tires in the experimental data are slightly higher than the longitudinal slip data obtained from the simulation responses particularly for the rear tires as seen in FIGURES 9(f) and (g). This is due to the fact that it is difficult for the driver to maintain a constant speed during maneuvering. In simulation, it is also assumed that the vehicle is moving on a flat road during step steer maneuver. In fact, it is observed that the road profiles of test field consist of irregular surface. This can be another source of deviation on longitudinal slip response of the tires.



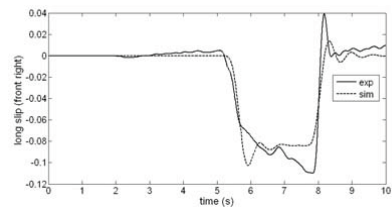
a) Vehicle speed



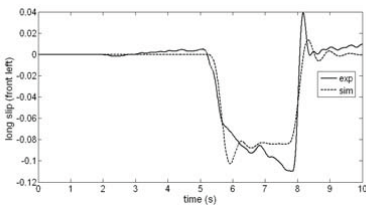
b) Longitudinal acceleration



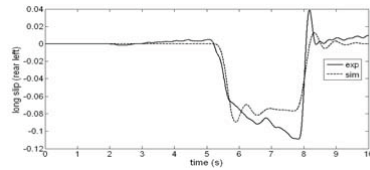
c) Pitch rate



d) Longitudinal slip front right



e) Longitudinal slip front left



f) Longitudinal slip rear left

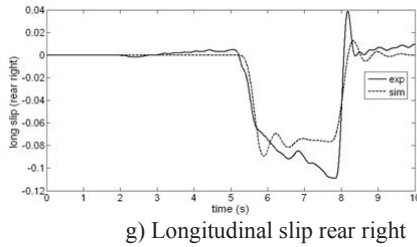
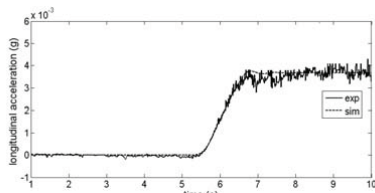
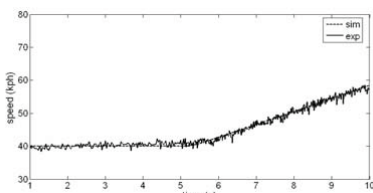


FIGURE 9: Response of the Vehicle for sudden braking test at constant speed of 60 kph

The results of Sudden Acceleration test at constant speed of 40kph indicate that measurement data and the simulation results agree with a relatively good accuracy as shown in FIGURE 10. FIGURE 10(a) shows the vehicle speed which is used as the input for the simulation model. In terms of pitch rate and longitudinal acceleration, it can be seen clearly that the simulation and experimental result are very similar with minor difference in magnitude as shown in FIGURE 10(b) and (c). The minor difference in magnitude and small fluctuation occurred on the measured data is due to the body's flexibility which was ignored in the simulation model. In terms of tire's longitudinal slip, the trends of simulation results show close agreement for both experimental data and simulation are shown in FIGURE 10(d), (e), (f) and (g). Closely similar to the validation results obtained from sudden acceleration test, the longitudinal responses of all tires in experimental data are smaller than the longitudinal slip data obtained from the simulation. Again, this is due to the difficulty of the driver to maintain a constant speed during sudden acceleration test maneuver. Assumption in simulation model that the vehicle is moving on a flat road during the maneuver is also very difficult to realize in practice. In fact, road irregularities of the test field may cause the change in tire properties during the vehicle handling test. Assumption of neglecting steering inertia may possibility lower down the magnitude of tire longitudinal slip in simulation results compared with the measured data.



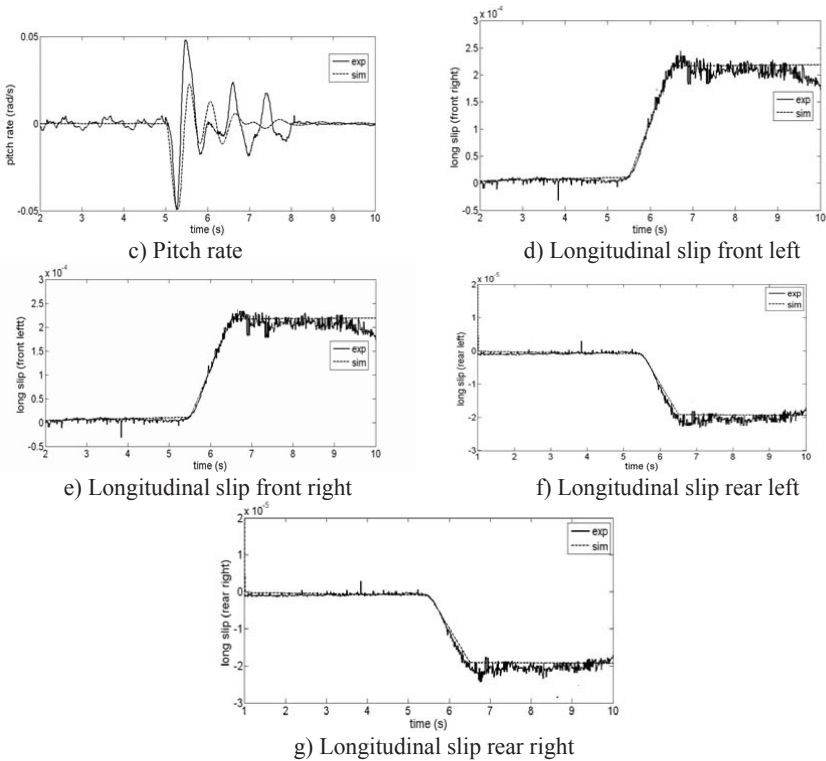


FIGURE 10: Response of the vehicle for sudden acceleration test at constant speed 40 kph

5.0 PERFORMANCE EVALUATION OF GSPID CONTROL

The performance of GSPID controller is examined through simulation studies using SIMULINK toolbox of the MATLAB software package. For comparison purposes, the performance of the GSPID is compared with both the conventional PID control approach and passive system. The performance of the controller is examined through vehicle translational motion namely body pitch angle, pitch rate, body acceleration and body displacement.

5.1 Simulation Parameters

The simulation study was performed for a period of 10 seconds using Heun solver with a fixed step size of 0.01 second. The controller parameters are obtained using trial and error technique. The numerical values of the 14-DOF full vehicle model parameters and Calspan tire model parameters as well as the controller parameters are shown in Table 2:

TABLE 2: Tire parameter

Parameter	FWD radial
Tire designation	P185/70R13
T_w	7.3
T_p	24
F_{zT}	980
C_1	1.0
C_2	0.34
C_3	0.57
C_4	0.32
A_o	1068
A_1	11.3
A_2	2442.73
A_3	0.31
A_4	-1877
K_a	0.05
CS/FZ	17.91
μ_o	0.85

5.2 Step Change Test Driver Input

To predict the performance of APID controller, a step function driver input test is applied. The tests consist of sudden braking test and sudden acceleration test. In sudden braking test, the vehicle is accelerated and maintained to a nominal speed of 70 kph, then 6MPa brake is applied to hold the pressure firmly until the vehicle stopped completely. For the remainder of the simulation, the steering is maintained constantly at zero degree appropriately. In sudden acceleration test, the same condition is applied to the vehicle, and then full step throttle input is applied to make the vehicle accelerate immediately. In order to fulfill the objective of designing the active suspension system, there are four parameters observed in the simulations. The four parameters are the vehicle body acceleration, body displacement, pitch rate and pitch angle. The solid lines are defined as the active suspension under APID controller, the dashed lines are describe as the active suspension under PID controller and the dotted lines are label of the passive system response.

From FIGUREs 11(a) and (b), the pitch behavior for the APID controller indicates better performance reduced dive during the maneuver compared to conventional PID. It is shown in the vertical acceleration plot. The APID made the vehicle lose the momentum during the maneuvers and reduced the vehicle weight transfer to the front. FIGURE 11(c) illustrates clearly how the APID can effectively absorb the vehicle's vibration in comparison to active suspension under PID controller and

the passive suspension system. The oscillation of the body acceleration using the APID system is much reduced significantly, which guarantees better ride comfort and reduce of body vertical displacement as shown in FIGURE 11(d).

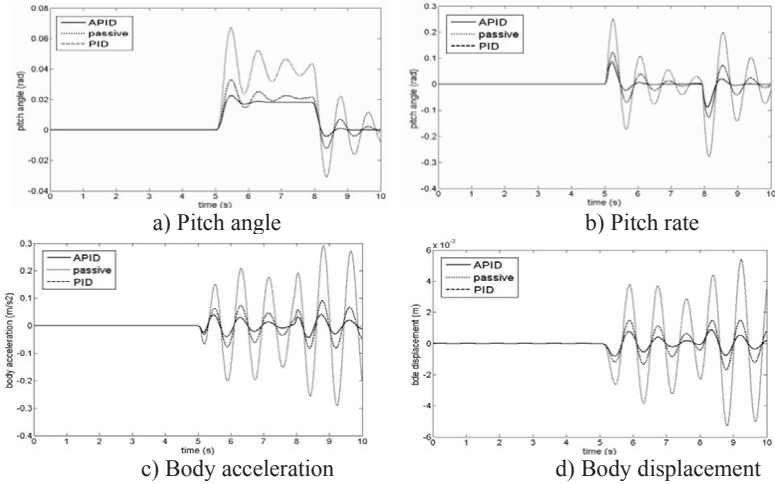
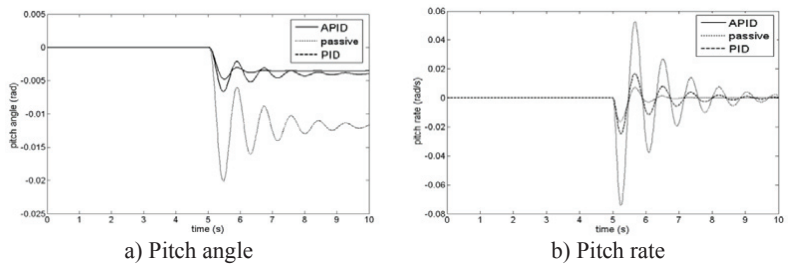


FIGURE 11: Performance of GSPID at step function brake 6 MPa

The results of the sudden acceleration test showed that the proposed controllers, APID are reasonably efficient methods in enhancing vehicle stability in term of reducing squat. In this case, the input of the vehicle is changed from braking to throttling input. FIGURE 12 show that performance of the APID controller has a good tracking performance with good transient response. FIGURE 12 (a) shows the response of the vehicle from sudden acceleration test maneuver which is input for the simulation model. In terms of the pitch rate, the proposed controller gives the system a more stable output when it is compared to PID structures as shown in FIGURE 12 (b). The result of the body acceleration and body displacement are shown in FIGURE 12 (c) and FIGURE 12 (d) respectively. The FIGURE explains that the APID controller gives better performance in terms of settling time and reducing the magnitude as compared to the counterparts..



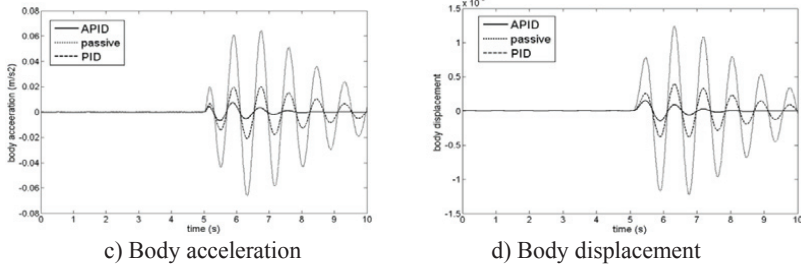
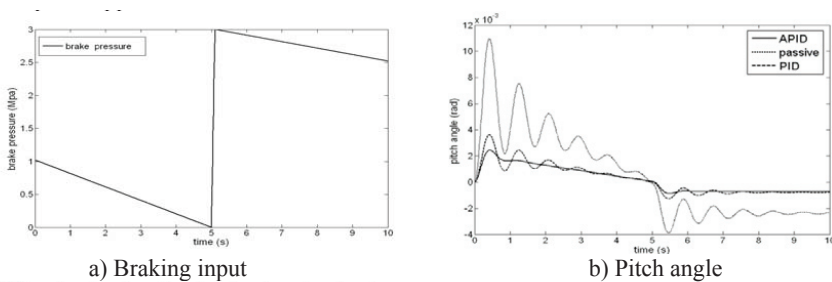


FIGURE 12: Performance of GSPID at step function full throttle

5.3 Response Of The Controller For Unbounded Signal

To verify the robustness of the controller, a similar test is conducted for unstable driver input out of predetermined range. The test used unstable brake pressure as the input of the sudden braking test and unstable throttle push as the input of the sudden acceleration test. FIGURE 13 (a) shows the braking input which is used as the input for the sudden braking test. The result is clearly explained that the simulation under APID controller is yielded very effectively to enhance vehicle stability and ride quality in terms of reducing vehicle dive as shown in FIGURE 13 (b). The major difference in magnitude and small fluctuation occurred in the graph is due to the flexibility of the APID to adapt with the condition held on the system which shows in pitch rate plot in FIGURE 13 (c). In terms of body acceleration as shown in FIGURE 13 (d), the trends of simulation results show the APID significantly improve with better performance as compared to the conventional PID. Due to the improvement of the body acceleration, the magnitude of the body displacement is reduced. FIGURE 13 (e) shows the evidence on the vehicle remains steady even when the unstable driver input is applied.



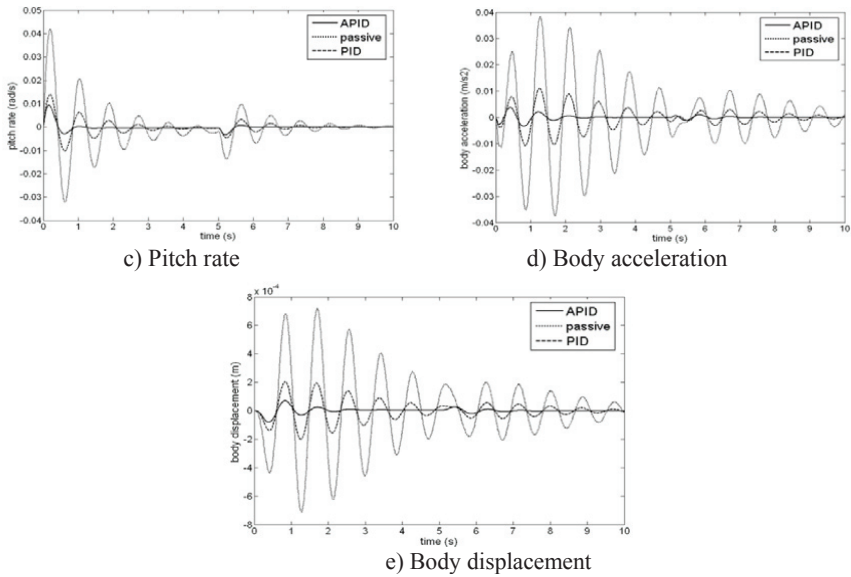


FIGURE 13: Performance of GSPID at unbounded braking input

The performance of APID controller is then observed using unstable throttle input. The simulation test needs the vehicle to accelerate in a constant speed of about 20kph, and then the inconstant throttle input is applied as shown in FIGURE 14(a). In this case, the reference position and pitch are remained at zero degree respectively. The responses of the vehicle are described in FIGURES 14(b) to (e). FIGURES 14(b) and (c) explain on the performance of APID in reducing the pitch angle and pitch rate which, as a result, is able to decrease the vehicle squat. In addition, the magnitude of body acceleration (FIGURE 14(d)) and the body displacement (FIGURE 14 (e)) of the vehicle are visibly reduced. Overall, it can be said that the proposed controller has a good performance, stable and has good transient response in tracking of the system and can adapt with the stated range and the value in between the stated range held on sudden braking test or sudden acceleration test. The comparison between the APID and the conventional PID controller presents that the proposed schemes are much more effective in improving the stability of the vehicle during sudden acceleration and braking condition. As a result, the controller is verified to be able to enhance better vehicle performance and riding quality as shown in the simulation responses.

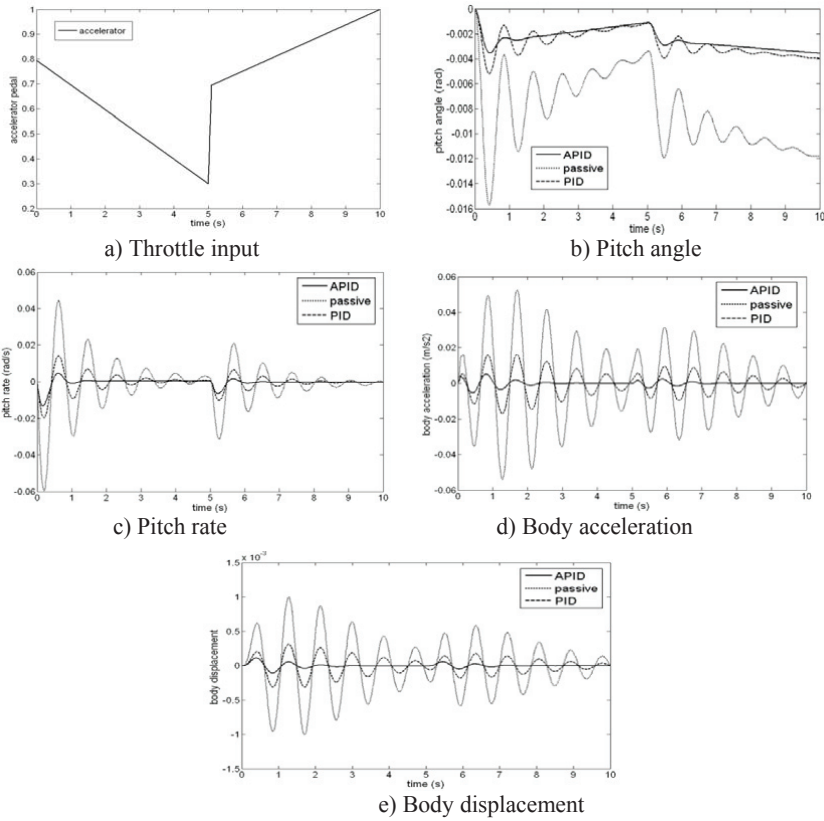


FIGURE 14: Performance of GSPID at unbounded throttle input

6.0 CONCLUSION

An adaptive PID controller with pitch moment rejection for vehicle dive and squat to enhance vehicle stability and ride quality has been evaluated. The proposed controller which includes the proportional, integral and derivative gains are allowed to vary within predetermined range of the sudden braking and sudden acceleration tests. Simulation studies for an active suspension with validated full vehicle model are presented to demonstrate the effectiveness of using the APID controller. Two types of simulation tests namely sudden braking test and sudden acceleration test have been performed and data gathered from the tests were used as the benchmark of the proposed verification. Some of the vehicle's behaviors observed in these works are pitch rate, pitch angle, body acceleration and body displacement responses. The performance characteristics of the controller are evaluated and compared with conventional PID. The result shows that the use of the proposed APID control technique proved to be effective in controlling vehicle pitch and

vibration and achieve better performance than the conventional PID controller.

7.0 ACKNOWLEDGEMENT

This work is supported by the Ministry of Science Technology and Innovation (MOSTI) through its scholarship and financial support and Ministry of Higher Education (MoHE) of Malaysia through FRGS project entitled "Development of a Pneumatically Actuated Active Stabilizer Bar to Reduce Unwanted Motion In Longitudinal Direction" lead by Dr. Khisbullah Hudha at Universiti Teknikal Malaysia Melaka. This financial support is gratefully acknowledged.

8.0 REFERENCE

- Ahmad, F., Hudha, K., Said. M. R. and Rivai. A. (2008a). Development of Pneumatically Actuated Active Stabilizer Bar to Reduce Vehicle Dive. Proceedings of the International Conference Plan Equipment and Reliability. March 27-28. Kuala Lumpur, Malaysia
- Ahmad, F., Hudha, K., Said. M. R. and Rivai. A. (2008b). Development of Pneumatically Actuated Active Stabilizer Bar To Reduce Vehicle squat. Proceedings of the 3rd Brunei International Conference on Engineering and Technology 2008. November 2-5. Bandar Sri Begawan, Brunei Darussalam
- Ahmad, F., Hudha, K. Rivai. A. and Zakaria, M. M. N. (2008c). Modeling And Validation of Vehicle Dynamic Performance in Longitudinal Direction. Submitted to Journal Of Advanced Manufacturing (JAMT).
- Bahouth, G. (2005). Real World Crash Evaluation of Vehicle Stability Control (VSC) Technology. 49th Annual Proceedings Association for the Advancement of Automotive Medicine. September 12-14. Boston, Massachusetts, America
- Campos, J., Davis, L., Lewis, F., Ikanega, S., Scully, S. and Evans, M. (1999). Active Suspension System Control of Ground Vehicle Heave and Pitch Motions. Proceedings of the 7th IEEE Mediterranean Control Conference on Control and Automation. June 28-30. Haifa, Israel.
- Chantranuwathana, S. (2001). Adaptive Robust Force Control for Vehicle Active Suspensions. University of Michigan. Ph.D. Dissertation

- Chantranuwathana, S. (2001). Adaptive Robust Force Control for Vehicle Active Suspensions. IEEE Proceeding of the American Control Conference. June, San Diego, California. pp. 1702-1706
- Donahue, M. D. (2001). Implementation Of An Active Suspension, Preview Controller For Improve Ride Comfort. Master Thesis University of California, Barkeley.
- Fenchea, M. (2008). Influence of Car's Suspension in the Vehicle Comfort and Active Safety. Annals of the University of Oradea, Fascicle of Management and Technology Engineering. Vol. VII (XVII) pp. 791-796
- Fialho, I and. Balas, G. J. (2002). Road Adaptive Active Suspension Design Using Linear Parameter Varying Gain-Scheduling. IEEE Transactions on Control System Technology. Vol. 10, No. 1, pp. 43-51.
- Gao, B., Darling, J., Tilley, D. G. and Williams, R.A. (2006). Modeling and Simulation of a Semi-active Suspension System. Department of Mechanical Engineering, University of Bath, Bath a.d Engineering Centre, Jaguar and Land Rover, Whitely, Coventry,
- Hudha, K., Kadir, Z., Jamaluddin, H. (2008). Modeling , Validation and Roll Moment Rejections Control for Pneumatically Actuated Active Roll Control for Improving Vehicle Lateral Dynamics Performance. Accepted for Publication in International Journal Engineering System Modeling and Simulation (IJESMS) with serial number Vol. 1, No. 2.
- Hudha, K., Jamaluddin, H. Samin, P. M. and Rahman, R. A. (2003). Semi Active Roll Control Suspension System on a New Modified Half Car Model. SAE Technical Paper Series. Paper No. 2003-01-2274.
- Ikanega, S. and Lewis, F. L., Campos, J. and Davis, L. (2000). Active Suspension Control of Ground Vehicle Based on a Full-Vehicle Model. Proceeding of the American Control Conference on Ground Vehicle Based. Chicago, Illinois, USA. June 28-30. Vol. 6, pp.4019-4024.
- Kadir, Z. A., Hudha, K., Nasir, M. Z. M. and Said, M. R. (2008). Assessment of Tire Models for Vehicle Dynamics Analysis. Proceedings of the International Conference on Plant Equipment and Reliability. March 27-28. Kuala Lumpur, Malaysia.
- Kasprzak, E. M. and Gentz, D. (2006) The Formula SAE® Tire Testing Consortium - Tire Testing and Data Handling. SAE Technical Paper. (2006-01-3606)
- Kasprzak, E. M., Lewis, K. Eand Milliken, D. L. (2006). Modeling Tire Inflation Pressure Effects in the Nondimensional Tire Model. SAE Technical

Paper. Paper No. (2006-01-3607)

- Karnopp, D. (1995). Active and Semi-active Vibration Isolation. *Journal of Mechanical Design*, ASME. Vol.177, pp. 177-185.
- Kruczek, A. and Stribrsky, A. (2004). A Full-car Model for Active Suspension – Some Practical Aspects', *Proceedings of the IEEE International Conference on Mechatronics*. June 3-5. Istanbul Turkey. pp. 41-45.
- Labaryade, R. and Aubert, D. (2003). A Single Framework for Vehicle Roll, Pitch, Yaw Estimation and Obstacles Detection by Stereovision. *Proceedings IEEE on Intelligent Vehicles Symposium*. June 9-11. Columbus, USA. pp. 31-36.
- Lee, C. H., Shin, M. H. and Chung, N. J. (2001). A Design of Gain-Scheduled Control for a Linear Parameter Varying System: An Application to Flight Control. *Control Engineering Practice* 9, pp. 11-21
- March, C. and Shim, T. (2007). Integrated Control of Suspension and Front Steering to Enhance Vehicle Handling. *Proc. IMeche. Journal of Automobile Engineering*. vol. 221, No. 152, pp, 377-391.
- Sam, Y. M. and Osman, J. H. S. (2006). Sliding Mode Control of a Hydraulically Actuated Active Suspension. *Jurnal Teknologi, Universiti Teknologi Malaysia*. Vol.3, No.44, pp.37-48
- Sam, Y. M. and Osman, J. H. S (2005). Modeling and Control of the Active Suspension System Using Proportional Integral Sliding Mode Approach. *Asian Journal of Control*. Vol. 7, No. 2, pp, 91-98.
- Mailah, M. and Priyandoko, G. (2007). Simulation of a Suspension System with Adaptive Fuzzy Active Force Control. *International Journal of Simulation Modeling*. 6 (1). pp. 25-36. ISSN 1726-4529
- SAE J266. (1996). Steady-State Directional Control Test Procedures for Passenger Cars and Light Trucks. SAE International Publication. Jan 1.
- Sampson, D.J.M., Jeppesen, B.P. and Cebon, D. (2000). The Development of an Active Roll Control System for Heavy Vehicles. In *Proceedings of 6th International Symposium on Heavy Vehicle Weights and Dimensions*. pp. 375–384. June18-22, Saskatoon, Saskatchewan, Canada.
- Sampson, D. J. M. (2002). Active Roll Control of Articulated Heavy Vehicles, Technical Report CUED/C-MECH/TR 82, Department of Engineering, University of Cambridge, UK,

- Sampson, D.J.M. and Cebon, D. (2003a). Achievable Roll Stability of Heavy Road Vehicles. Proc. Instn Mech. Engrs, Part : J. Automobile Engineering. 217(4), pp. 269–287.
- Sampson, D.J.M. and Cebon, D. (2003b) Active roll control of single unit heavy road vehicles Vehicle System Dynamics, 40 (4). pp. 229-270. ISSN 0042-3114
- Sedaghati, A. (2006). API Controller Based on Gain-Scheduling for Synchronous Generator. Turkish Journal of Electrical Engineering and Computer Sciences. Vol.14, No.2. pp. 241-251
- Singh, T., Kesavadas, T., Mayne, R., Kim, J. J. and Roy, A. (2002). Design of Hardware/Algorithms for Enhancement of Driver-vehicle Performance in Inclement Weather Conditions Using a Virtual Environment. SAE 2004 Transactions Journal of Passenger Car: Mechanical Systems. Paper No. 2002-01-0322.
- Stilwell, D. J. and Rugh, W. J. (1999). Interpolation of Observer State Feedback Controllers for Gain Scheduling. IEEE Transactions on Automatic Control. Vol. 44, No. 6, pp. 1225-1229.
- Szostak, H. T., Allen, W. R. and Rosenthal, T. J. (1988). Analytical Modeling of Driver Response in Crash Avoidance Maneuvering Volume II: An Interactive Model for Driver/Vehicle Simulation. US Department of Transportation Report NHTSA DOT HS-807-271. April.
- Toshio, Y. and Atsushi, T. (2004). Pneumatic Active Suspension System for a One-Wheel Car Model Using Fuzzy Reasoning and a Disturbance Observer. Journal of Zhejiang University SCIENCE. Vol. 5, No. 9, pp. 1060-1068.
- Toshio, Y. and Itaru, T. (2005). Active Suspension Control of a One-wheel Car Model Using Single Input Rules Modules Fuzzy Reasoning and a Disturbance Observer. Journal of Zhejiang University SCIENCE. Vol.6A, No. 4, pp. 251-256.
- Vaughan, J., Singhose, W. and Sadegh, N. (2003). Use of Active Suspension Control to Counter the Effects of Vehicle Payloads. Proceeding of IEEE Conference on Control Applications, 2003 Istanbul, (CCA 2003). June 23-25. Istanbul, Turkey. Vol. 1 pp. 285-289.
- Wang, F.C. and Smith, M.C. (2002). Active and Passive Suspension Control for Vehicle Dive and Squat. In: Johansson, R. and Rantzer, A., (eds.) Nonlinear and Hybrid Systems in Automotive Control. Springer-Verlag. London, UK. pp. 23-39. ISBN 1852336528.

Weeks, D. A., Beno, J. H., Guenin, A. M. and Breise, D. A. (2000). Electromechanical Active Suspension Demonstration for Off Road Vehicles. SAE Technical Paper Series. Vol.01, No.0102.

Yoshimura, T., Isari, Y., Li, Q. and Hino, J. (1997a). Active Suspension of Motor Coaches Using Skyhook Damper and Fuzzy Logic Controls. Control Engineering Practice. Vol. 5, No. 2, pp. 175-184.

Yoshimura, T., Nakaminami, K. and Hino, J. (1997b). A Semi-active Suspension with Dynamic Absorbers of Ground Vehicles Using Fuzzy Reasoning. International Journal of Vehicle Design, Vol. 18, No. 1, pp. 19-34.

Yoshimura, T., Hiwa, T., Kurimoto, M. and Hino, J. (2003). Active Suspension of a One-wheel Car Model Using Fuzzy Reasoning and Compensators. International Journal of Vehicle Autonomous Systems, Vol. 1, No. 2, pp. 196-205.

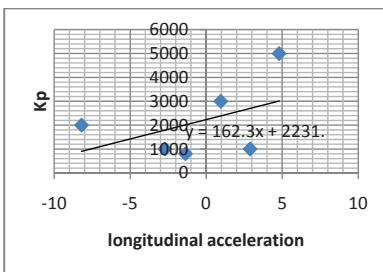
Yoshimura, T. and Watanabe, K. (2003). Active Suspension of a Full Car Model Using Fuzzy Reasoning Based on Single Input Rule Modules with Dynamic Absorbers', International Journal of Vehicle Design, Vol. 31, No. 1, pp. 22-40.

Yoshimura, T., Kume, A., Kurimoto, M. and Hino, J. (2001). Construction of An Active Suspension System of a Quarter Car Model Using the Concept of Sliding Mode Control. Journal of Sound and Vibration, Vol. 239, No. 2, pp. 187-199

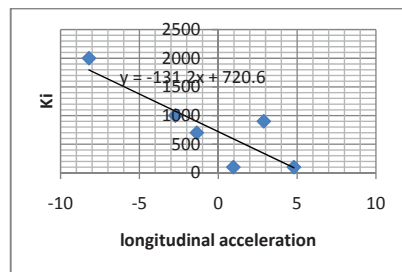
Zhang, Y., Zhao, L., Cong, H. and Wang, B. (2004). Study on Control of Vehicle Attitude and Ride Comfort Based on Full-car Model. Fifth World Congress on Intelligent Control and Automation, 2004. (WCICA 2004). Vol.4, pp. 3514- 3519. June 15-19, Hangzhou, China.

APPENDIXES

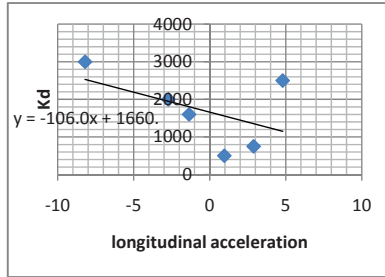
Controller Parameters for Body Bounce (F_z)



(a): Kp value

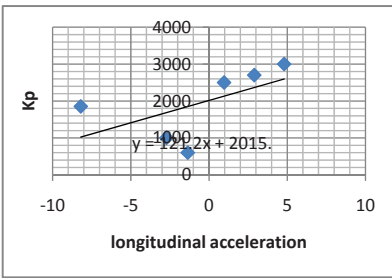


(b): Ki value

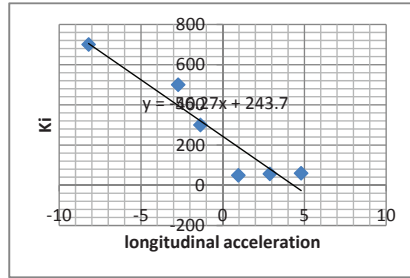


(c): Kd Value

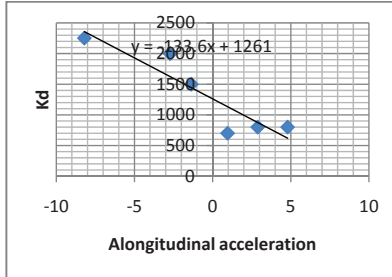
Controller Parameters for Body Pitch (M_q)



(a): Kp value



(b): Ki value



(c): Kd value